Journal of Organometallic Chemistry 695 (2010) 2658–2666

Contents lists available at ScienceDirect

Journal of Organometallic Chemistry

journal homepage: www.elsevier.com/locate/jorganchem

Metallacrown ethers with a symmetric bis(phosphite) ligand derived from 1,2-bis-(2-hydroxyethoxy)benzene: Synthesis, characterization and hydroformylation of styrene

Abha A. Kaisare [a], Samuel B. Owens Jr. [a], Edward J. Valente [b,1], Gary M. Gray [a,*]

[a] Department of Chemistry, University of Alabama at Birmingham, 901 14th Street South, Birmingham, AL 35294-1240, USA
[b] Department of Chemistry & Biochemistry, Mississippi College, 200 South Capitol Street, Clinton, MS 39056, USA

ARTICLE INFO

Article history:
Received 25 May 2010
Received in revised form
7 August 2010
Accepted 10 August 2010
Available online 18 August 2010

Keywords:
Metallacrown ether
Conformational restraint
Bis(phosphite)
Hydroformylation

ABSTRACT

To better understand the effects of ligand configuration on hydroformylation reactions carried out in the presence of $LiBPh_4 \cdot 3dme$ (dme = 1,2-dimethoxyethane), a conformationally restrained bis(phosphite) ligand derived from 1,2-bis-(2-hydroxyethoxy)benzene, $\{[(2,2'\text{-}O_2C_{12}H_8)P(C_2H_4O_2)]_2C_6H_4\}$, **1**, has been prepared and its Rh(I) metallacrown ether complex has been evaluated as a catalyst for the hydroformylation of styrene. Both the activity and regioselectivity of the catalyst are sensitive to the amount of the $LiBPh_4 \cdot 3dme$ added with the activity decreasing by 16% and the regioselectivity for the *iso* increasing by 9% at a 8:1 $LiBPh_4$:Rh ratio.

Model complexes for the octahedral, *cis*-$Mo(CO)_4$(**1**), **2**, and square planar, *cis*-$PtCl_2$(**1**), **3**, and *cis*-$PdCl_2$(**1**), **4**, complexes in the catalytic cycle has been have been studied using multinuclear NMR spectroscopy and X-ray crystallography. Although the X-ray crystal structure of **2** suggests that the metallacrown ether ring could adopt a configuration capable of binding alkali metal cations, this does not appear to occur in a dichloromethane-d_2 solution of **2** because no shift in the ^{31}P NMR resonance **2** is observed upon the addition of an excess of $LiBPh_4 \cdot 3dme$. The $^{31}P\{^1H\}$ NMR spectra of chloroform-*d* solutions of **2** (in the presence of a catalytic amount of $HgCl_2$) and of **4** and the X-ray crystal structures of the complexes indicate that the bis(phosphite) ligands are *cis* coordinated in these complexes in both the solution and in the solid state. This is particularly surprising for **4** because related $PdCl_2\{Ph_2P(CH_2CH_2O)_nCH_2CH_2PPh_2\}$ ($n = 3–5$) complexes exhibit both *cis–trans* and monomer–oligomer equilibria in solution.

1. Introduction

We have recently demonstrated that both the rates and regioselectivities of alkene hydroformylation reactions catalyzed by phosphite and bis(phosphite) ligands can be affected by the presence of alkali metal salts [1,2]. The mechanism by which this occurs is not currently known. The binding of the hard alkali metal cations is known to activate carbonyl ligands towards nucleophilic attack and to weaken the metal-carbonyl bond [3–8], which would facilitate migratory–insertion reactions [9,10] in the catalytic cycle. Cation binding to carbonyl ligands could also affect the equilibria between five-coordinate reservoir species and four-coordinate active intermediates for the alkene coordination and H_2 oxidative-addition steps.

We have also previously reported that metallacrown ether complexes with bis(phosphine)-, bis(phosphinite)- and bis(phosphite) polyether ligands [11–15] are able to form complexes in which hard metal cations are coordinated to the ether oxygens. Thus it is of interest to determine if the cation binding abilities of these ligands would have any effect on the catalytic activities and selectivities of their Rh(I) complexes in the alkene hydroformylation.

As one step in answering this question, we have carried out a study of the hydroformylation of styrene with Rh(I) metallacrown ether complexes containing a conformationally restrained bis(phosphite) ligand derived from 1,2-bis-(2-hydroxyethoxy)benzene. The effects of various amounts of $LiBPh_4 \cdot 3dme$ (dme = 1,2-dimethoxyethane) on the activities and regioselectivities of the catalysts have also been studied. We have chosen this ligand for the catalytic studies for two reasons. The first reason is that in recent years, rhodium complexes of rigid and sterically constrained bis(phosphite) ligands and phosphine-phosphite hybrid ligands have receive considerable attention due to their remarkable

* Corresponding author. Tel.: +1 205 934 8094; fax: +1 205 934 2543.
E-mail address: gmgray@uab.edu (G.M. Gray).
[1] Present address: University of Portland, Swindells Hall, 5000 N Willamette Blvd, Portland, OR 97203, USA.

0022-328X/$ – see front matter © 2010 Elsevier B.V. All rights reserved.
doi:10.1016/j.jorganchem.2010.08.010

activities and selectivities [16–25]. The second reason is the ligand has similar phosphite groups to those used in our previously reported hydroformylation results that were carried out either with a Rh(I) catalyst containing a sterically constrained bis(phosphite) ligand derived from tartaric acid [1] or with monodentate phosphite-ether ligands [2] under reactions identical conditions as shown in Fig. 1.

We have also synthesized and characterized Mo(0), Pd(II), Pt(II) model complexes of the ligand to gain more insight into the structural features of the sterically constrained bis(phosphite) ligand. The model complexes may resemble the octahedral and square planar complexes in the catalytic complexes and hence complement the catalytic studies. The implications of the NMR spectroscopic data as to the solution conformations of the complexes are discussed. X-ray crystal structures of the Mo(0) and Pd(II) complexes have been determined, and the important features of the conformations of the metallacrown ether rings in these complexes are evaluated.

2. Experimental section

2.1. Materials and methods

All reactions and purification procedures were carried out under dry nitrogen. All starting materials were reagent grade and were used as received. Tetrahydrofuran (THF) was first distilled from calcium hydride and then from sodium/benzophenone and stored over molecular sieves. Triethylamine was distilled from sodium/benzophenone prior to use. 1,2-bis(2-hydroxyethoxy)benzene was dried azeotropically using toluene. Deuterated NMR solvents (chloroform-*d*, dichloromethane-d_2) were opened and handled under a nitrogen atmosphere at all times. $LiBPh_4 \cdot 3dme$ was purchased from Aldrich and used as received. Literature procedures were used to prepare *cis*-$Mo(CO)_4$(nbd), 2,2′-biphenylylenephosphochloridite ester, 1,2-bis(2-hydroxyethoxy)benzene, $Rh(CO)_2$ (acac) and $PtCl_2$(cod) [26–29].

All $^{31}P\{^1H\}$, $^{13}C\{^1H\}$ and ^1H NMR spectra of the ligands and complexes were recorded using a Bruker DRX-400 NMR spectrometer. The $^{13}C\{^1H\}$ and the ^1H NMR spectra were referenced to internal $SiMe_4$ while the $^{31}P\{^1H\}$ NMR spectra were referenced to external 85% phosphoric acid. Quantitative $^{31}P\{^1H\}$ NMR spectra were obtained with an inverse gated 30° pulse sequence and a delay of 10 s between pulses. Elemental analyses were performed by Atlantic Microlabs, Norcross, GA.

2.2. Synthesis of {[(2,2′-$O_2C_{12}H_8$)P($C_2H_4O_2$)]$_2C_6H_4$}, **1**

A solution of 0.760 g (3.84 mmol) of 1,2 bis-(2-hydroxy ethoxy) benzene, 1.92 g (7.68 mmol) of 2, 2′- biphenylylenephosphochloridite ester and 1.07 mL (7.68 mmol) of triethylamine in 150 mL of freshly distilled THF was stirred under nitrogen for 12 h at ambient temperature. The mixture was then filtered through diatomaceous earth, and the filtrate was evaporated to dryness to yield 1.84 g (76.6%) of crude **1** as viscous, colorless oil. $^{31}P\{^1H\}$ NMR (chloroform-*d*): δ 140.04 (s). ^1H NMR (chloroform-*d*): δ 4.10 (t, 4H, $|^3J(HH)|$ 4.4 Hz, $C\underline{H}_2OPh$), δ 4.27–4.30 (m, 4H, $C\underline{H}_2OP$), δ 6.87 (bs, 4H, ArH), δ 7.09–7.45 (m, 16H, ArH).

2.3. Synthesis of cis-Mo(CO)$_4${[(2,2′-$O_2C_{12}H_8$)P($C_2H_4O_2$)]$_2C_6H_4$}, **2**

A solution of 0.12 g (0.41 mmol) of $Mo(CO)_4$(nbd) and 0.26 g (0.41 mmol) of **1** in 100 mL of degassed dichloromethane was

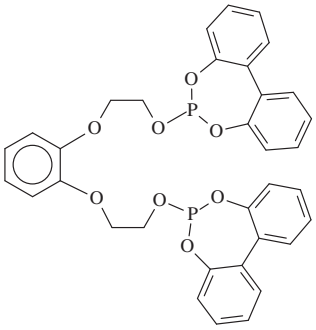

1

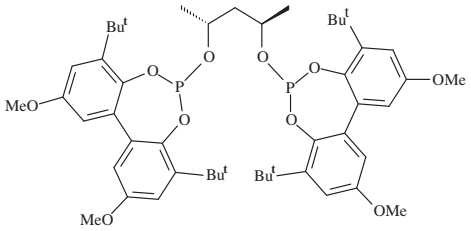

5

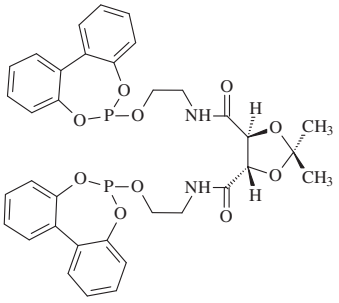

6

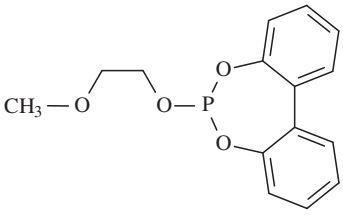

7

Fig. 1. Ligands used in the hydroformylation of styrene [1,2].

stirred for 1 h at ambient temperature resulting in a pale yellow solution. A $^{31}P\{^{1}H\}$ NMR spectrum of the reaction mixture was then taken and exhibited a single resonance of the product complex indicating that the reaction was complete. The solution was then evaporated to dryness to yield 0.25 g (73%) of crude **2** as an off white powder. The crude product was purified by recrystallization from a dichloromethane-hexanes mixture to give analytically pure **2** as colorless crystals. Anal. Calcd for $C_{38}H_{28}O_{12}P_2Mo$: C, 54.68; H, 3.36. Found: C, 54.99; H, 3.54. $^{31}P\{^{1}H\}$ NMR (chloroform-*d*): δ 169.16 (s). ^{1}H NMR (chloroform-*d*): δ 4.16–4.18 (m, 4H, $\underline{CH_2}OPh$), 4.30–4.31 (m, 4H, $\underline{CH_2}OP$), 6.93–7.50 (m, 20H, Ar$\underline{H}$). $^{13}C\{\underline{^{1}H}\}$ NMR (carbonyl and aliphatic carbons, chloroform-*d*): δ 211.33 (*trans* $\underline{C}O$ aq, $|^{2}J(PC) + {}^{2}J(P'C)|$ 33 Hz), 206.60 (*cis* $\underline{C}O$, t, $|^{2}J(PC)|$ 14 Hz), 69.79 (s, $\underline{C}H_2OAr$), 66.14, 6(aq, $|^{2}J(PC) + {}^{4}J(P'C)|$ 5 Hz, $\underline{C}H_2OP$).

2.4. Synthesis of cis-$PtCl_2\{[(2,2'\text{-}O_2C_{12}H_8)P(C_2H_4O_2)]_2C_6H_4\}$, **3**

A solution of 0.40 g (1.1 mmol) of $PtCl_2$(cod) and 0.69 g (1.1 mmol) of **1** in 100 mL of degassed dichloromethane was stirred for 2 h at ambient temperature, and then the solution was evaporated to dryness to yield 0.79 g (81%) of crude **7** as a white residue. The crude product was purified by recrystallization from a tetrahydrofuran-hexanes mixture to give analytically pure **2** as a colorless crystalline powder. Anal. Calcd for $C_{34}H_{28}O_8P_2Cl_2Pt$: C, 45.73; H, 3.13. Found: C, 45.83; H, 3.19. $^{31}P\{^{1}H\}$ NMR (chloroform-*d*): δ 83.44 (s, $|^{1}J(PtP)|$ 5873 Hz). ^{1}H NMR (chloroform-*d*): δ 4.18 (t, 4H, $|^{3}J(HH)|$ 4.1 Hz, $\underline{CH_2}OPh$), δ 4.74–4.79 (m, 4H, $\underline{CH_2}OP$), 7.05–7.39 (m, 20H, Ar$\underline{H}$). $^{13}C\{\underline{^{1}H}\}$ NMR (aliphatic carbons, chloroform-*d*) δ 69.44, (s, $\underline{C}H_2OAr$), 68.46, (bs, $\underline{C}H_2OP$).

2.5. Synthesis of cis-$PdCl_2\{[(2,2'\text{-}O_2C_{12}H_8)P(C_2H_4O_2)]_2C_6H_4\}$, **4**

A mixture of 0.18 g (1.0 mmol) of $PdCl_2$ in 50 mL of acetonitrile was stirred at ambient temperature for 24 h under nitrogen to yield a light yellow solution of $PdCl_2(MeCN)_2$. The solution was then transferred into 100 ml Schlenk flask containing 0.63 g (1.0 mmol) of **1** in 25 mL of acetonitrile. The reaction mixture was stirred for 1 h under nitrogen. Then, it was filtered and the filtrate evaporated to dryness to yield 0.58 g (72%) of crude **4** as greenish yellow powder. The crude product was purified by recrystallization from a dichloromethane-hexanes mixture to give analytically pure **4** as yellow crystals. $^{31}P\{^{1}H\}$ NMR (dichloromethane-d_2): δ 108.96 (s). ^{1}H NMR (dichloromethane-d_2): δ 4.18 (t, 2H, $|^{3}J(HH)|$ 4.0 Hz, $\underline{CH_2}OPh$), δ 4.82 (bs, 2H, $\underline{CH_2}OP$), δ 6.92–7.27(m, 8H, Ar$\underline{H}$). $^{13}C\{^{1}H\}$ NMR (aliphatic carbons, dichloromethane-d_2) δ 70.08, (s, $\underline{C}H_2OP$) δ 68.23, (s, $\underline{C}H_2OAr$).

2.6. $HgCl_2$-catalyzed cis–trans isomerization of cis-$Mo(CO)_4\{[(2,2'\text{-}O_2C_{12}H_8)P(C_2H_4O_2)]_2C_6H_4\}$, **2**

A solution of 0.021 g (0.025 mmol) of **2** in 0.5 ml of chloroform-*d* was prepared in a 5 mm, screw-top NMR tube under nitrogen, and the $^{31}P\{^{1}H\}$ NMR spectrum of the solution was recorded. Then, a catalytic amount of solid $HgCl_2$ was added to the solution. After 2 min of vigorous shaking, a $^{31}P\{^{1}H\}$ NMR spectrum was taken. Additional $^{31}P\{^{1}H\}$ NMR spectra were taken over a period of two months to monitor the reaction and showed only the starting material: δ 170.95 (s).

2.7. X-ray structural analyses of cis-$Mo(CO)_4\{(2,2'\text{-}O_2C_{12}H_8)P(C_5H_6O_2)_2P(2,2'\text{-}O_2C_{12}H_8)\}$, **2** and $PdCl_2\{(2,2'\text{-}C_{12}H_8O_2)PO(CH_2CH_2OCH_3)_2\}$, **4**

Hot, saturated dichloromethane-hexanes solutions of **2** and **4** were slowly cooled to yield X-ray quality single crystals of each complex. A suitable single crystal of **2** was glued on a glass fiber with epoxy and aligned on an Enraf Nonius CAD4 single crystal

Table 1
Crystal structure data and refinement data for **2** and **4**.

	2	**4**
CCDC#	773040	773041
Empirical formula	$C_{38}H_{28}O_{12}P_2Mo$	$C_{34}H_{28}Cl_2O_8P_2Pd$
Formula weight	834.48	803.80
Temperature	293(2) K	298(2) K
Wavelength	0.71073 Å	0.71073 Å
Crystal system	Triclinic	Orthorhombic
Space group	P-1	$P2_1$
Unit cell dimensions	$a = 10.597(2)$ Å	$a = 9.94417(11)$ Å
	$b = 11.505(2)$ Å	$b = 17.5296(2)$ Å
	$c = 15.703(3)$ Å	$c = 19.3262(3)$ Å
	$\alpha = 94.65(3)^\circ$	$\alpha = 90^\circ$
	$\beta = 104.40(3)^\circ$	$\beta = 90^\circ$
	$\gamma = 102.33^\circ$	$\gamma = 90^\circ$
Volume	1793.4(6) Å^3	3368.90(7) Å^3
Z	2	4
Density (calculated)	1.545 Mg/m^3	1.585 Mg/m^3
Absorption coefficient	0.520 mm^{-1}	0.855 mm^{-1}
F(000)	848	1624
Crystal size	0.30 × 0.40 × 0.45 mm^3	0.63 × 0.48 × 0.12 mm^3
Theta range for data collection	2.04–22.48°	3.16–30.62°
Index ranges	$-11 \le h \le 11$, $-1 \le k \le 12$, $-16 \le l \le 16$	$-14 \le h \le 14$, $25 \le k \le 24$, $-27 \le l \le 27$
Reflections collected	5532	33685
Independent reflections	4686 [R(int) = 0.0668]	10058 [R(int) = 0.0231]
Completeness to theta$_{max}$°	100.0%	98.6%
Absorption correction	Empirical	Analytical
Max. and min. transmission	0.4562 and 0.3944	0.9043 and 0.6148
Refinement method	Full-matrix least squares on F^2	Full-matrix least squares on F^2
Data/restraints/parameters	4648/0/478	10058/0/424
Goodness-of-fit on F^2	1.082	1.009
Final R indices [I > 2sigma(I)]	$R1 = 0.0477$, wR2 = 0.1184	$R1 = 0.0400$, wR2 = 0.0818
R indices (all data)	$R1 = 0.0682$, wR2 = 0.1290	$R1 = 0.0507$, wR2 = 0.0887
Largest diff. peak and hole	1.142 and −0.416 e·Å^{-3}	0.626 and −0.412 e·Å^{-3}

Table 2
Selected bond lengths (A°), bond angles (°) and torsion angles (°) for **2** and **4**.

2		**4**	
P(1)–Mo	2.4249(14)	P(1)–Pd	2.2289(8)
P(2)–Mo	2.4464(16)	P(2)–Pd	2.2261(9)
C(35)–Mo	2.032(6)	Cl(1)–Pd	2.3248(11)
C(36)–Mo	1.984(6)	Cl(2)–Pd	2.3363(11)
C(37)–Mo	2.038(6)		
C(38)–Mo	2.031(6)		
C(35)–O(9)	1.127(6)		
C(36)–O(10)	1.137(6)		
C(37)–O(11)	1.132(6)		
C(38)–O(12)	1.131(7)		
P(1)–Mo–P(2)	89.40(5)	P(2)–Pd–P(1)	96.52(3)
C(35)–Mo–P(1)	175.44(15)	P(2)–Pd–Cl(1)	85.10(4)
C(36)–Mo–P(1)	90.22(15)	P(1)–Pd–Cl(1)	169.72(4)
C(37)–Mo–P(1)	86.26(14)	P(2)–Pd–Cl(2)	175.60(4)
C(38)–Mo–P(1)	91.63(17)	P(1)–Pd–Cl(2)	86.62(4)
C(35)–Mo–P(2)	95.13(15)	Cl(1)–Pd–Cl(2)	92.36(5)
C(36)–Mo–P(2)	179.68(15)		
C(37)–Mo–P(2)	89.04(15)		
C(38)–Mo–P(2)	87.52(16)		
C(11)–C(16)–C(17)–C(22)	40.9(7)	C(11)–C(16)–C(17)–C(22)	40.0(6)
C(23)–C(28)–C(29)–C(34)	−41.9(8)	C(23)–C(28)–C(29)–C(34)	−42.2(6)
C(35)–Mo–P(2)–O(4)	−112.8(2)	Cl(1)–Pd–P(2)–O(4)	−39.32(13)
C(36)–Mo–P(1)–O(1)	−89.2(2)	Cl(2)–Pd–P(1)–O(1)	77.99(16)

diffractometer under aerobic conditions. Standard peak search and automatic indexing routines followed by least squares fits of 25 accurately centered reflections resulted in accurate unit cell parameters. The space group of the crystal was assigned on the basis of systematic absences and intensity statistics. Details of the data collection of each complex are given in Table 1. The analytical scattering factors of the complex were corrected for both $\Delta f'$ and $i\Delta f''$ components of anomalous dispersion. All data were corrected for the effects of absorption and for Lorentz and polarization effects.

All crystallographic calculations were performed with the Siemens SHELXTL-PC program package [30]. The metal and P positions were located using the Patterson method and the remainder of the non-hydrogen atoms were located in difference Fourier maps. Full-matrix refinement of the positional and anisotropic thermal parameters for all non-hydrogen atoms versus F^2 was carried out. All hydrogen atoms were placed in calculated positions with the appropriate molecular geometry and the δ (C–H) = 0.96 Å. The isotropic thermal parameter associated with each hydrogen atom was fixed equal to 1.2 times the U_{eq} of the atom to which it was bound.

A suitable crystal of **4** was attached to the tip of a 0.1 mm diameter glass capillary and mounted on a goniometer head. The crystallographic properties and data were collected using MoKα radiation and the charge-coupled area detector (CCD) on an Oxford Diffraction Systems Gemini diffractometer at 298(2) K. A preliminary set of cell constants was calculated from reflections observed on three sets of 5 frames that were oriented approximately in mutually orthogonal directions of reciprocal space. Data collection was carried out using MoKα radiation (graphite monochromator) with 11 runs consisting of 473 frames with a frame time of 39.9 s, and a crystal-to-CCD distance of 50.000 mm. The runs were collected by omega and phi scans of 1.0° width, and at detector position of −30.187 and 28.624° in 2θ. The intensity data were corrected for absorption with an analytical correction. Final cell constants were calculated from 20561 stronger reflections from the actual data collection after integration.

Selected bond lengths, bond angles and torsion angles for complexes **2** and **4** are given in Table 2. Crystallographic data for all complexes has been deposited with the Cambridge Crystallographic Database (**2**: CCDC 773040 **4**: CCDC 773041).

2.8. Hydroformylation of styrene

The hydroformylation reactions were carried out using a Parr Series 4560 minireactor connected to a high-pressure gas burette, which introduced gas to the reactor at a constant pressure. The digitized reactor temperature, burette temperature, and burette pressure were monitored using Agilent Benchlink Data Logger software on a PC connected to an Agilent data acquisition switch unit. In

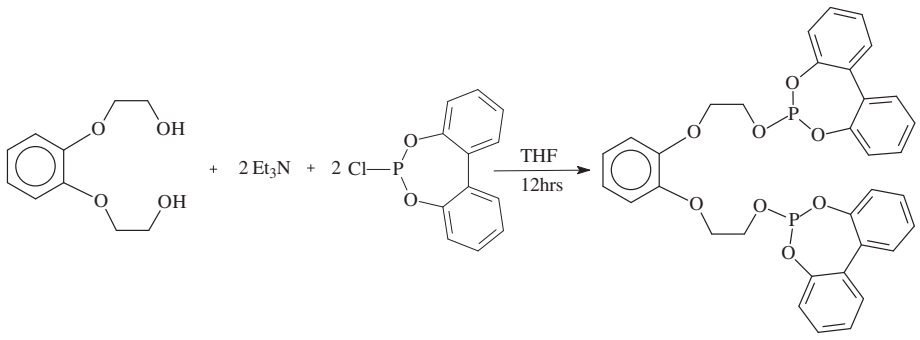

Scheme 1. Synthesis of ligand **1**.

Table 3
Catalytic Data for the Hydroformylation of Styrene using Rh(I) Complexes of Ligand **1**.

	1[a]		**6**[b]		**5** (Chiraphite®)[b]		**7**[c]	
$LiBPh_4$:Rh	k (s^{-1})	% iso/% *n*	k (s^{-1})	% iso/% *n*	k (s^{-1})	% iso/% *n*	k (s^{-1})	% iso/% *n*
None	1.9×10^{-4}	76/24	3.4×10^{-4}	80/20	5.0×10^{-4}	90/10	3.5×10^{-4}	75/25
4:1	1.6×10^{-4}	83/17	2.7×10^{-4}	85/15			2.1×10^{-4}	86/14
8:1	1.5×10^{-4}	86/14	3.0×10^{-4}	87/13			6.7×10^{-4}	86/14
32:1	8.4×10^{-5}	77/23	3.2×10^{-4}	86/14	5.0×10^{-4}	97/3	5.1×10^{-4}	87/13

[a] All numbers reported in the table are the average of those from two runs under identical conditions. Conditions (all ratios are molar): $CO/H_2 = 1{:}1$, $T = 80$ °C P (CO/H_2) = 20 atm, substrate/Rh = 1000, k (s^{-1}) at ligand/Rh = 1.2. No hydrogenation was observed. % iso/% n ratio was determined when pressure change was no longer observed using ^1H NMR. The differences in the % iso and % n were less than 2% for duplicate runs.% Conversion of styrene was greater than 99%. The pseudo first order rate constant (k) was obtained from a first order fit of pressure drop vs. time using Graphical Analysis software [31]. The difference in the k values was less than 10% for duplicate runs. The coefficient of variation was 5.8% for the k values, 0.22% for the % iso values and 0.90% for the % n values.
[b] Data from reference 1.
[c] Data from reference 2.

a typical run, a solution of $Rh(CO)_2(acac)$ and the alkali metal salt, if used, in 12 mL of dry THF and a solution of **1** in 10 mL of dry THF were separately added to the reactor via needle transfer under nitrogen pressure through the substrate inlet valve. Next, the reactor was purged three times with a 1:1 H_2:CO gas (syngas) mixture and then pressurized to 20 atm with syngas and heated to 80 °C with mechanical stirring. The reactor was maintained under these conditions for 45 min to allow for pre-catalyst equilibration and then was cooled to 30 °C before the pressure was vented. Styrene (0.0337 mol) was then injected into the reactor through the substrate inlet valve, after which the reactor was pressurized to 20 atm with syngas and heated to 80 °C. The reaction progress was then monitored using the Agilent software. The data obtained from pressure drop versus time was fitted using Graphical Analysis version 3.4 [31] using an exponential function to determine the pseudo first order rate constant.

3. Results and discussion

3.1. Ligand synthesis and NMR characterization of {[(2,2′-$O_2C_{12}H_8$)P($C_2H_4O_2$)]$_2C_6H_4$}, *1*

The ligand, **1**, was prepared by the reaction of 1,2-bis-(2-hydroxyethoxy)benzene with 2,2′-biphenylylenephosphochloridite ester in THF in the presence of triethylamine as shown in Scheme 1. The NMR spectra of **1** show no unexpected features. The $^{31}P\{^1H\}$ NMR resonance is a singlet. The chemical shift of the $^{31}P\{^1H\}$ NMR resonance is close to those of other phosphite and bis(phosphite) ligands [2,32,33] derived from the 2,2′-biphenylylenephosphochloridite ester. The ^1H NMR spectrum of the ligand exhibits two resonances in the 4.09–4.30 ppm region, indicating that the protons attached to each methylene carbon are chemically equivalent. No attempt was made to assign these resonances. Because the $^{31}P\{^1H\}$, ^1H NMR spectra of the crude ligand contained no unexpected resonances, it was used in the syntheses of metal complexes and in the catalytic studies.

3.2. Hydroformylation of styrene using a Rh(I) complex of *1*

Previous studies have demonstrated that both the activities and regioselectivities of the hydroformylations of styrene (Fig. 1), which has a preference for the *iso*-aldehyde, catalyzed by Rh(I) complexes of bis-(phosphite) ligands are sensitive to the presence of alkali metal salts [1] as shown by the data summarized in Table 3. For each set of reaction conditions, two catalytic runs were carried out. The differences in the rate constants were less than 10% and differences in the % iso and % n were less than 2% for the duplicate runs. The coefficients of variance for the fitted k (s^{-1}) and % iso/% n values were determined from these values for all of the sets of catalytic conditions and were 5.8% for k (s^{-1}), 0.22% for the % iso and 0.90% for % n values. When the catalyst was a Rh(I) complex of Chiraphite®, **5**, the regioselectivity increased in the presence of $LiBPh_4$, but the activity remained constant. In contrast, when the catalyst was a Rh(I) complex of a tartrate-derived bis(phosphite), **6**, the activity decreased slightly upon addition of $LiBPh_4$, but the regioselectivity improved, with the best regioselectivity being observed at an 8:1 mol ratio of $LiBPh_4$:Rh. In the absence of $LiBPh_4$, the Rh(I) complex of **1** is both less active and less regioselective than that of **6**. However, at an 8:1 mol ratio of $LiBPh_4$:Rh(I), the two catalysts have essentially the same regioselectivity although the Rh(I) complex of **6** is still more active. These results clearly demonstrate that the nature of the bridging group in the bis(phosphite) ligand has a significant effect on both the catalytic activity and regioselectivity of the Rh(I) complex in the alkene hydroformylation.

It is also interesting that the addition of $LiBPh_4$ has quite different effects on the catalytic activities and regioselectivities of a Rh(I) complex of the phosphite ligand **7** [2]. At a **7**:Rh ratio of 2.5:1, which gives essential the same Rh to phosphite donor group ratio as does the 1.2:1 ratio used with the bis(phosphite) ligands, the addition of $LiBPh_4$ (8:1 $LiBPh_4$:Rh) increases both the activity (the pseudo first order rate constant increases 3.5×10^{-4} to 6.7×10^{-4}) and the regioselectivity (% iso/% *n* increases from 76/24 to 85/15) [2]. Although the increase in regioselectivity for the Rh(I) complex of **7** is similar to that seen with the Rh(I) complex of **1** at 8:1 $LiBPh_4$:Rh, the increase in the pseudo first order rate constant is quite different. It is not certain why the activities of the Rh(I) complexes of bis(phosphite)s and phosphites are affected so differently by the addition of $LiBPh_4$, although one possibility is that the phosphites may occupy different coordination sites on the Rh than do the bis(phosphite)s. It is well established that the equatorial–equatorial or equatorial-apical preferences of bis

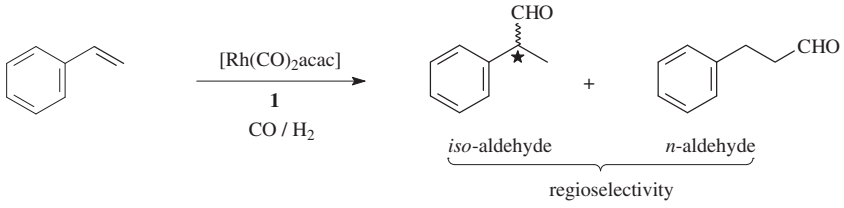

Scheme 2. Hydroformylation of styrene using ligand **1**.

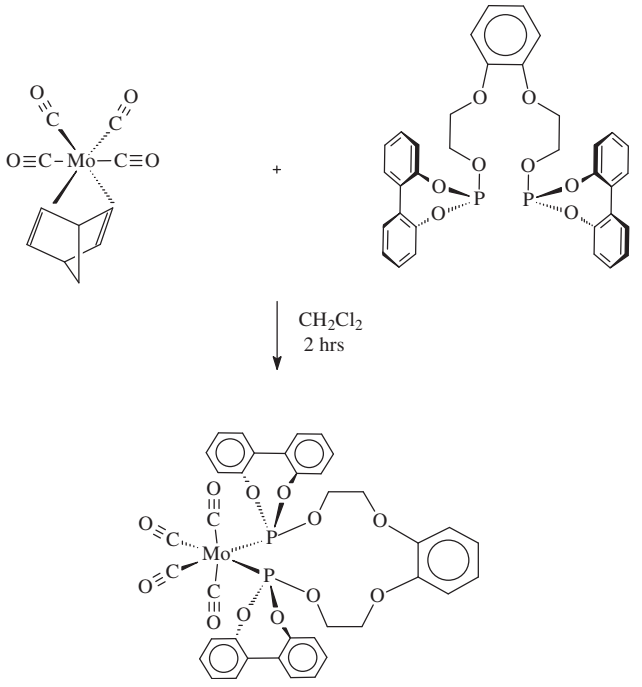

Scheme 3. Synthesis of complex **2**.

(phosphite) ligands have significant effects on the regioselectivities of their Rh(I) hydroformylation catalysts [34]. Whatever the reason, it is quite clear that seemingly minor changes in the ligands have significant effects on the activities of the Rh(I) complexes in the hydroformylation of styrene (Scheme 2).

3.3. Syntheses and NMR characterizations of model complexes of *1*

Model complexes of **1**, have been synthesized and characterized by $^{31}P\{^1H\}$, $^{13}C\{^1H\}$ and ^1H NMR spectroscopy to better understand the effect of the variation in transition metal center on the solution conformations of metallacrown ether and the abilities of the metallacrown ethers to bind alkali metal cations [15]. Model octahedral and square planar complexes of **1**, are complementary to the catalytic studies because they may resemble intermediates in the catalytic hydroformylation reaction and therefore may provide insight for optimizing the metallacrown ether for the hydroformylation reaction.

The *cis*-$Mo(CO)_4\{[(2,2'\text{-}O_2C_{12}H_8)P(C_2H_4O_2)]_2C_6H_4\}$, **2**, octahedral model complex was prepared as shown in Scheme 3. As has previously been observed for other complexes of type *cis*-$Mo(CO)_4$(P-donor ligand)$_2$ [35], the $^{31}P\{^1H\}$ NMR of **2** displays a single resonance at 169.16 ppm which is approximately 29 ppm downfield of that of the free ligand indicating that only the *cis* isomer of **2** is present. The two well-resolved $^{13}C\{^1H\}$ resonances for the carbonyls in chloroform-*d* further support the proposed *cis* coordination geometry for the complex. The downfield resonance, due to carbonyls *trans* to phosphites, is an apparent quintet (A portion of an AXX′ spin system) [36] whereas the upfield resonance, due to carbonyls *trans* to carbonyls, is a 1:2:1 triplet (A portion of an AX_2 spin system).

The position of the $^{31}P\{^1H\}$ NMR resonance does not appreciably change when a 61 fold excess of $LiBPh_4 \cdot 3dme$ is added to the dichloromethane-d_2 solution. This suggests that the complex **2** binds to Li^+ cations very weakly in dichloromethane-d_2 solution. Given that the styrene hydroformylation reactions were run in tetrahydrofuran, which is a much more strongly coordinating solvent that is dichloromethane, it seems unlikely that cation binding to the metallacrown ether ring is occurring in the catalyst intermediates.

As discussed previously, one difference between the bis(phosphite) and phosphite ligands that have been used in the hydroformylation catalysts is that they could have different preferences for coordination sites in the catalytic intermediates. To compare the coordination preferences of the bis(phosphite) ligand, **1**, with that of the phosphite ligand, **7**, the $HgCl_2$-catalyzed *cis*–*trans* isomerization of **2**, was followed by $^{31}P\{^1H\}$ NMR spectroscopy to determine the *cis*–*trans* preference of **1** in an octahedral complex. Even after two months, only the *cis* isomer is observed in solution. This is in contrast to the $HgCl_2$ catalyzed isomerization of *cis*-$Mo(CO)_4(\mathbf{7})_2$ in which a 46:54 *cis*–*trans* ratio is observed at equilibrium [2]. The very different *cis*–*trans* ratios for the two ligands demonstrates that the steric constraints in the bis(phosphite) ligand backbone have a significant effect on the coordination preference of the ligand.

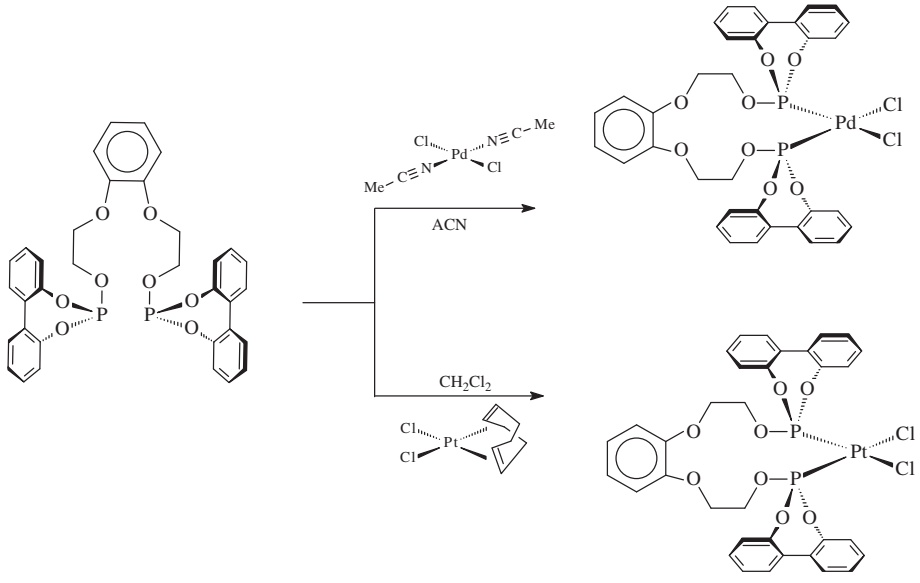

Scheme 4. Synthesis of complex **3** and **4**.

The *cis*-$PtCl_2\{[(2,2'\text{-}O_2C_{12}H_8)P(C_2H_4O_2)]_2C_6H_4\}$, **3**, square planar model complex was prepared as shown in Scheme 4. The single $^{31}P\{^1H\}$ NMR resonance of this complex and the magnitude of $^1J(PtP)$ are consistent with the *cis* arrangement of phosphorus donor groups at the platinum [37].

The *cis*-$PdCl_2\{[(2,2'\text{-}O_2C_{12}H_8)P(C_2H_4O_2)]_2C_6H_4\}$, **4**, conformationally restrained square planar model complex was prepared as shown in Scheme 4. In contrast to the $^{31}P\{^1H\}$ NMR spectra of the previously reported and closely related $PdCl_2\{Ph_2P(CH_2CH_2O)_n CH_2CH_2PPh_2\}$ (n = 3, 4, 5) metallacrown ethers, which exhibit singlet resonances due to the *cis* and *trans* geometrical isomers of both monomeric and cyclic oligomeric complexes at equilibrium [38,39], the $^{31}P\{^1H\}$ NMR spectrum of the complex **4** in dichloromethane-d_2 exhibits a single singlet resonance. The coordination geometry of the ligand in **4** was determined by X-ray crystallography as discussed below.

3.4. X-ray crystal structures of model complexes **2** and **4**

The X-ray crystal structures of **2** and **4** have been determined, and the molecular structures are shown in Figs. 2 and 3 respectively. These structures are of interest because they allow the effect the variation in transition metal center on the conformation of metallacrown ether ring to be examined and are closely related to the previously reported structures of sterically hindered and symmetrical metallacrown ethers [40]. The solid state conformations of **2** and **4** also provide insight into the catalytic studies because they allow the metallacrown ether ring conformations to be evaluated for their potential abilities to bind alkali metal cations.

Consistent with the NMR data, **2** has a *cis* octahedral coordination geometry similar to that seen in other *cis*-$Mo(CO)_4$(P-donor ligand)$_2$ complexes. As compared to the previously reported *cis*-$Mo(CO)_4$(P-donor ligand)$_2$ complexes [2,41,42], the octahedron is not significantly distorted as indicated by the small deviation of the phosphorus-molybdenum-phosphorus bond angle (89.40(5)°) from the ideal angle of 90°.

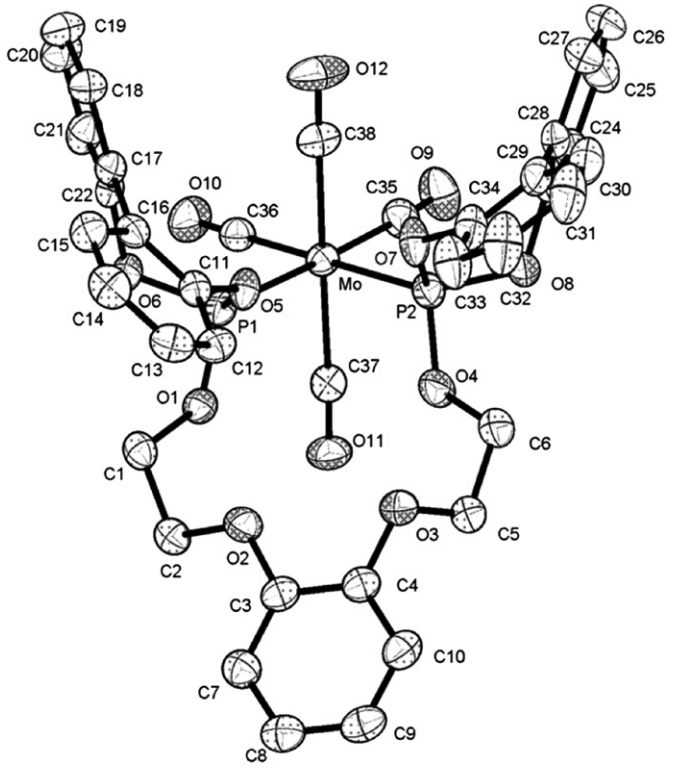

Fig. 2. ORTEP drawing of the molecular structure of 2. The hydrogens are omitted for clarity, and the thermal ellipsoids are drawn at the 50% probability level.

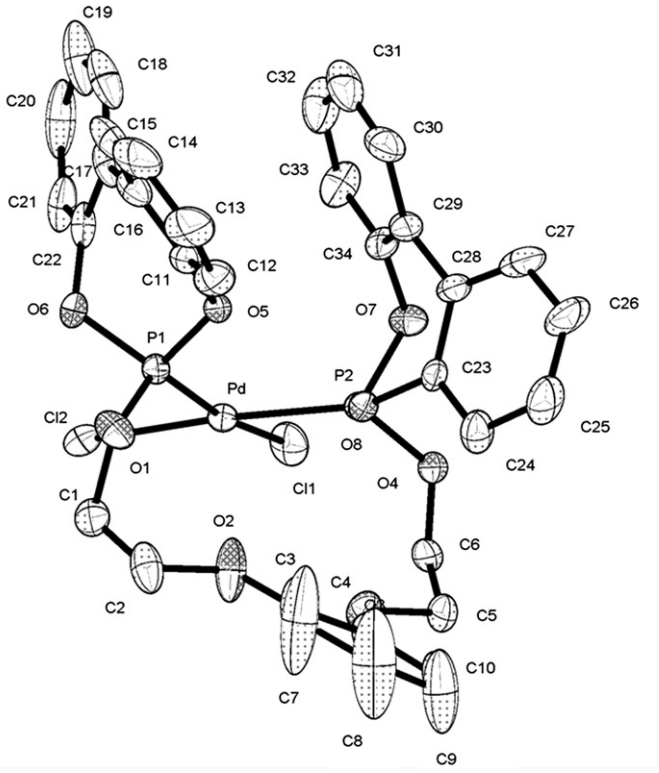

Fig. 3. ORTEP drawing of the molecular structure of 4. The hydrogens are omitted for clarity, and the thermal ellipsoids are drawn at the 50% probability level.

The coordination geometry of the palladium in **4** is a distorted square plane composed of two *cis* chlorines and two *cis* phosphites. This geometry is surprising because similar $PdCl_2$(P-donor ligand)$_2$ complexes in which the P-donor ligand is a phosphine are generally equilibrium mixtures of *cis* and *trans* isomers with the equilibrium strongly favoring the *trans* isomer [38,39]. The fact that a single $^{31}P\{^1H\}$ NMR resonance is observed suggests that the complexes maintain the *cis* coordination geometry in the solution as well as in the solid state. The distortion in the phosphorus-palladium-phosphorus angle (96.52(3)°) is significantly larger in **4** than in **2** and may be due to different crystal packing forces arising from the very different metallacrown ether ring conformations and coordination geometries in the two complexes.

The metallacrown ether ring in **2** is almost symmetric due to a pseudo mirror plane that bisects the phenylene ring and the molybdenum center. This pseudo symmetric structure has all four of the ring oxygen atoms (O1, O2 O3, O4) pointed into the ring, which should be a favorable position for cation binding. However, two ring oxygens, O1 and O4, point below the least squares plane

Table 4
Distances (A°) from the centroid of O(1), O (2), O(3),O(4), O(5), O(7) for **2**.

O(1)	2.438
O(2)	2.514
O(3)	2.473
O(4)	2.062
O(5)	2.098
O(7)	2.813

through O1, O2, O3 and O4 while the other two oxygen atoms, O2 and O3, point above the least squares plane. The relative orientation and the size of the cavity created by O1, O2, O3, O4, O5 and O7 suggest that a Li^+ could fit into the cavity easily but not a Na^+ because the average distance of O1, O2, O3, O4, O5 and O7 from the centroid is 2.3996 Å (Table 4), which is greater than the sum of the ionic radii of lithium and van der Waals radii of oxygen atom but smaller than the sum of the ionic radii of sodium and van der Waals radii of oxygen atom. This suggests that this metallacrown ether could exhibit size selectivity for alkali metal cation binding. However, as discussed above, there is no evidence of cation binding in the $^{31}P\{^1H\}$ NMR experiments, which suggests that this conformation is not a low energy solution conformation, that other factors are inhibiting cation binding or that the $^{31}P\{^1H\}$ NMR chemical shift is not sensitive to cation binding. It is interesting that *cis*-Mo$(CO)_4(\{Ph_2P(CH_2CH_2O)_2\}_2$-*o*-$C_6H_4)$ [40], which also has an *o*-phenylene group in the metallacrown ether ring fails to exhibit cation binding although the related metallacrown ether in which the *o*-phenylene is replaced by an ethylene, *cis*-Mo$(CO)_4(\{Ph_2P(CH_2CH_2O)_4CH_2CH_2PPh_2)$ [43] does bind Li^+ and Na^+ cations under the same conditions.

An metallacrown ether ring in **2** has a chair conformation. The four ring oxygen atoms, O1, O2 O3 and O4, form the seat of the chair and are nearly coplanar (O4: 0.0523 Å, O1: −0.0561 Å, O2: 0.0831 Å, O3: −0.0793 Å, mean deviation 0.0677 Å). The two phosphorus atoms are below the plane of oxygen atoms (P1: −1.170 Å, P2: −0.8551 Å) while phenylene group is above the plane of oxygen atoms (C3: 0.5681 Å, C4: 0.4693 Å, C7: 1.1031 Å, C10: 0.8830 Å, C8: 1.4955 Å, C9: 1.3966 Å).

An interesting feature of the structure of **2** is the orientation of one of the axial carbon monoxide ligands relative to the ring. This carbon monoxide is oriented so that it lies above the metallacrown ether ring and both the carbon and oxygen atoms are relatively close to the centroid of the cavity formed by O1, O2, O3, O4, O5 and O7 (distances of C37 and O11 from the centroid of the cavity formed by O1, O2, O3, O4, O5 and O7 are 3.443 Å and 3.856 Å respectively). This suggests that it should be possible for an alkali metal cation in the cavity to interact with the π-electrons of the triple bond if not with the nonbonding pair of electrons on the oxygen.

In contrast to **2**, the metallacrown ether ring in **4** adopts an asymmetric structure in which the rotations of the phosphepin groups about the P–Mo bonds are quite different as indicated by the torsion angles in Table 2. The oxygen atoms in this conformation do not point into the metallacrown ether ring suggesting that this conformation would not favor cation binding.

The biphenyl groups have similar conformations in the two complexes despite the differences in the conformations of the metallacrown ether rings. The absolute magnitudes of all of the torsion angles about the central C–C bonds in the biphenyls are quite similar. They are also similar to those observed for complexes with other bis(phosphepin) ligands [41] suggesting that the conformations of the seven-membered 1,3,2-dioxaphosphepin rings have a strongly preferred conformation. In addition, one torsion angle has a positive sign and one has a negative sign in each complex. Because the hands of the phosphepin rings can interconvert in solution, this suggests that the ligand conformation in which the two phosphepins have different hands may allow packing of the ligands in the *cis* coordination geometries at the metal centers that minimizes steric interactions between the phosphepin groups.

4. Conclusions

Rhodium (I) complexes of the bis(phosphite) ligand, **1** are active catalysts for the hydroformylation of styrene. The use of high concentrations of $LiBPh_4 \cdot 3dme$ (32:1 $LiBPh_4 \cdot 3dme$:Rh) lowers the activity without significantly improving in the regioselectivity of the catalyst while intermediate concentrations of $LiBPh_4 \cdot 3dme$ (4:1 or 8:1 $LiBPh_4 \cdot 3dme$:Rh) increase the regioselectivity of the catalyst while only slightly decreasing its activity.

Comparison of the hydroformylation results from this study with those previously reported with a Rh(I) catalysts containing either a tartaric acid–derived bis(phosphite) and a phosphite-ether ligand demonstrate that the activity of the catalysts are quite sensitive to the nature of the ligand backbone even though all the ligands provide significant conformational freedom. In contrast, the regioselectivities of the catalysts are quite similar, especially in the presence an optimal amount of $LiBPh_4 \cdot 3dme$. However, a detailed understanding of the effects chain length, steric bulk of the phosphite substituents, and number of oxygen atoms of the bis (phosphite) ligand on the activity and regioselectivity of their Rh(I) complexes as hydroformylation catalysts and on the abilities of their *cis*-Mo$(CO)_4$ complexes to bind alkali metal cations binding is still not available.

Ackowlegments

Support of this work by the University of Alabama at Birmingham and the NSF Cooperative Agreement EPS-0814103 is gratefully acknowledged. E. J. Valente gratefully acknowledges the support of NSF grant MRI 0618148 and the W. M. Keck Foundation for crystallographic resources.

References

[1] S.B. Owens Jr., G.M. Gray, Organometallics 27 (2008) 4282.
[2] A.A. Kaisare, S.B. Owens Jr., E.J. Valente, G.M. Gray, J. Organomet. Chem. 695 (2010) 1472 (and the references therein).
[3] J. Powell, M.R. Gregg, A. Kuksis, C.J. May, S.J. Smith, Organometallics 8 (1989) 2918.
[4] J. Powell, M.R. Gregg, P.E. Meindl, Organometallics 8 (1989) 2942.
[5] J. Powell, A. Lough, F. Wang, Organometallics 11 (1992) 2289.
[6] J. Powell, M.R. Gregg, A. Kuksis, C.J. May, J. Am. Chem. Soc. 103 (1981) 5941.
[7] J. Powell, M. Gregg, A. Kuksis, P.E. Meindl, J. Am. Chem. Soc. 105 (1983) 1064.
[8] J. Powell, A. Kuksis, C.J. May, P.E. Meindl, S.J. Smith, Organometallics 8 (1989) 2933.
[9] S.B. Butts, S.H. Strauss, E.M. Holt, R.E. Stimson, N.W. Alcock, D.F. Shriver, J. Am. Chem. Soc. 102 (1980) 5093.
[10] T.G. Richmond, F. Basolo, D.F. Shriver, Inorg. Chem. 21 (1982) 1272.
[11] G.M. Gray, F.P. Fish, C.H. Duffey, Inorg. Chim. Acta. 261 (1997) 233.
[12] C.H. Duffey, C.H. Lake, G.M. Gray, Inorg. Chim. Acta. 317 (2001) 199.
[13] D.C. Smith Jr., G.M. Gray, Inorg. Chem. 37 (1998) 1791.
[14] D.C. Smith Jr., C.H. Lake, G.M. Gray, Chem. Commun. 24 (1998) 2771.
[15] J.M. Butler, M.J. Jablonsky, G.M. Gray, Organometallics 22 (2003) 1081.
[16] A. Gual, C. Godard, C. Claver, S. Castillon, Eur. J. Org. Chem. 8 (2009) 1191.
[17] C.J. Cobley, R.D.J. Froese, J. Klosin, C. Qin, G.T. Whiteker, K.A. Abboud, Organometallics 26 (2007) 2986.
[18] T. Robert, Z. Abiri, J. Wassenaar, A.J. Sandee, S. Romanski, J.M. Neudoerfl, H.G. Schmalz, J.N.H. Reek, Organometallics 29 (2010) 478.
[19] M. Rubio, A. Suarez, E. Alvarez, C. Bianchini, W. Oberhauser, M. Peruzzini, A. Pizzano, Organometallics 26 (2007) 6428.
[20]. R. Abdallah, J.A.J. Breuzard, M.C. Bonnet, M. Lemaire, J. Mol. Catal. A: Chem. 249 (2006) 218.
[21] I. Odinets, T. Kegl, E. Sharova, O. Artyushin, E. Goryunov, G. Molchanova, K. Lyssenko, T. Mastryukova, G.V. Roeschenthaler, G. Keglevich, J. Organomet. Chem. 690 (2005) 3456.
[22] T.P. Clark, C.R. Landis, S.L. Freed, J. Klosin, K.A. Abboud, J. Am. Chem. Soc. 127 (2005) 5040.
[23] J. Klosin, C.R. Landis, Acc. Chem. Res. 40 (2007) 1251.
[24] K. Nozaki, H. Takaya, T. Hiyama, Top. Catal. 4 (1998) 175.
[25] I. Piras, R. Jennerjahn, R. Jackstell, W. Baumann, A. Spannenberg, R. Franke, K.D. Wiese, M. Beller, J. Organomet. Chem. 695 (2010) 479.
[26] L.V. Verizhnikov, P.A. Kirpichnikov, Zh. Obshch. Khim. 37 (1967) 1355.
[27] W. Ehrl, R. Rinck, H. Vahrenkamp, J. Organomet.Chem. 56 (1973) 285.
[28] Y.S. Varshavskii, T.G. Cherkasova, Zh. Obshch. Khim. 12 (1967) 1709.
[29] G. Topal, N. Demirel, T. Mahmut, Y. Turgut, H. Hosgoren, J. Heterocyclic. Chem. 38 (2001) 281.
[30] G.M. Sheldrick, SHELXTL NT ver.5. 10. Brucker AXS, Inc., Madison, WI, 1999.
[31] Graphical Analysis, 3.4, Vernier Software and Technology: Beaverton, OR, 2005.
[32] M. Hariharasarma, G.M. Gray, J. Organomet.Chem. 580 (1999) 328.
[33] M. Hariharasarma, C.L. Watkins, G.M. Gray, Organometallics 19 (2000) 1232.

[34] A. van Rooy, P.C.J. Kamer, P.W.N.M. van Leeuwen, N. Veldman, A.L. Spek, J. Organomet. Chem. 494 (1995) C15.
[35] G. Gray, Comments Inorg. Chem. 17 (1995) 95.
[36] D.A. Redfield, J.H. Nelson, L.W. Cary, Inorg. Nucl. Chem. Lett. 10 (1974) 727.
[37] A. Varshney, M.L. Webster, G.M. Gray, Inorg. Chem. 31 (1992) 2580.
[38] G.M. Gray, D.C. Smith, C.H. Duffey, Inorg. Chim. Acta 300 (2000) 581.
[39] D.C. Smith, G.M. Gray, Dalton 5 (2000) 677.
[40] C.H. Duffey, C.H. Lake, G.M. Gray, Organometallics 17 (1998) 3550.
[41] H. Byrd, J.D. Harden, J.M. Butler, M.J. Jablonsky, G.M. Gray, Organometallics 22 (2003) 4198 (and the references therein).
[42] J.M. Butler, G.M. Gray, J.P. Claude, Polyhedron 23 (2004) 1719.
[43] A. Varshney, G.M. Gray, Inorg. Chem. 30 (1991) 1748.